

# Performance Characterization Of Full Cell Lithium Ion Batteries With $\text{Na}_2\text{Li}_2\text{Ti}_6\text{O}_{14}$ As Anode And $\text{LiNi}_{0.8}\text{Mn}_{0.1}\text{Co}_{0.1}\text{O}_2$ (Nmc 811) As Cathode

Ramlan<sup>1</sup>, Titik Lestariningsih<sup>2</sup>, Achmad Subhan<sup>3</sup>, Akhmad Aminuddin Bama<sup>4</sup>, and Melenia Tambunan<sup>5</sup>

{ramlan@unsri.ac.id<sup>1</sup>, titi013@lipi.go.id<sup>2</sup>, achmo@brin.go.id<sup>3</sup>, akhmadbama@yahoo.com<sup>4</sup>, milen17022000@yahoo.com<sup>5</sup>}

Physics Department FMIPA University of Sriwijaya, Palembang, Indonesia<sup>1,4,5</sup>  
Pusat Riset Material Maju Badan Riset dan Inovasi Nasional (PRMM - BRIN), PUSPITEK, Tangerang Selatan, Indonesia<sup>2,3</sup>

Corresponding author: milen17022000@yahoo.com

**Abstract.** This lithium ion battery full cell is made with  $\text{Na}_2\text{Li}_2\text{Ti}_6\text{O}_{14}$  as the anode and NMC811 as the cathode. Lithium ion batteries are secondary batteries that can be recharged (rechargeable batteries), have good energy storage stability, high density and no memory effect. This research using the solid state reaction method, it was carried out by synthesizing the materials  $\text{Na}_2\text{Li}_2\text{Ti}_6\text{O}_{14}$  and  $\text{LiNi}_{0.8}\text{Mn}_{0.1}\text{Co}_{0.1}\text{O}_2$ , then the results of the synthesis were made into a slurry before coating and then the final stage was assembling for full cell coins of lithium ion batteries. After obtaining a full coin cell lithium ion battery, it was characterized using Electrochemical Impedance Spectroscopy, Charge-Discharge with a potential range of 1.5 V-3.5 V, cyclic voltammetry and XRD.

**Keywords :** Lithium ion batteries, full cell, charge-discharge, cyclic voltammetry

## 1 Introduction

The demand for *lithium ion batteries* increases every year for their energy storage capabilities and long life cycle, this is related to the increasingly rapid development of the electronics and telecommunications industry. Such as electric cars cell phones and tablet computers. Lithium ion batteries have electrical energy storage for a long period. However, the quality of the electrode (anode/cathode) can affect its properties. To increase and improve the performance of the battery, namely by improving the quality of the electrodes that will be used. The lithium ion battery itself has several constituent parts in the form of an anode, cathode and electrolyte. The current problem is that the cathode capacity is smaller than the anode capacity. So other materials are needed to increase the capacity of the cathode, one of which is nickel. The cathode used is nickel-manganese-cobalt (NMC). This is because NMC has the advantage that nickel has a higher synergy effect and increases capacity during charge-discharge.

Cobalt has the function of reducing the process of cation mixing caused by  $\text{Li}^+$  and  $\text{Ni}^{2+}$  ions because it has an atomic size that is almost the same as manganese which affects structural

stability [11]. NMC itself has many variations in its composition:  $\text{LiNi}_{0.8}\text{Mn}_{0.1}\text{Co}_{0.1}\text{O}_2$  (NMC 811) and  $\text{LiNi}_{0.8}\text{Mn}_{0.2}\text{Co}_{0.2}\text{O}_2$  (NMC 622), one of which has the largest nickel composition, namely NMC 811 and has the advantage of a larger capacity load. In 2025 the energy density is targeted to approach  $80\text{Wh Kg}^{-1}$  [2]. NMC 811 is included in the cathode target category desired by the automotive industry in the future, where the cathode material is included in the oxide conversion group which has advantages in terms of load capacity, output voltage and NMC conductivity level. Based on the EIS test from previous research, NMC 811 has a greater resistance than NMC 622 so its conductivity is smaller. Meanwhile, the diffusion value on the NMC 622 is much better than the NMC811. In NMC622 the diffusion value is  $4.18 \times 10^{-7}$  while for NMC 811 it is  $2.28 \times 10^{-7}$ , so NMC 622 has good lithium diffusion and a better conductivity level. However, the NMC 811 has a voltage of 0.56V, while the NMC 622 has a voltage of 0.25V, so that in the NMC 811 the *charge-discharge process* occurs and the capacity obtained is more reversible [6]. Therefore, this cathode material research focuses on NMC811 [8]. The basic working principle of lithium ion batteries is that in the charging process, when the battery is connected to a power source, the positive side of the power source will attract electrons and remove Li metal oxide, then the electrons will flow through the external circuit from the cathode to the anode and at the same time the lithium-ions also flow. through the electrolyte from the cathode to the anode, while in the discharge process when the battery is connected to a load, electrons and lithium-ions flow from the anode to the cathode.

## 2 Research methodology

This research was carried out in three stages. The first was the synthesis of the  $\text{Na}_2\text{Li}_2\text{Ti}_6\text{O}_{14}$  material using the solid state reaction method. Previously, a hydrothermal process was carried out by mixing 2.942 g of  $\text{NaHCO}_3$  as a source of Na, 1.294 g of  $\text{Li}_2\text{CO}_3$  as a source of Li and 8.392 g  $\text{TiO}_2$  as a Ti source which is expected to produce 10g  $\text{Na}_2\text{Li}_2\text{Ti}_6\text{O}_{14}$  formed. After obtaining the  $\text{Na}_2\text{Li}_2\text{Ti}_6\text{O}_{14}$  powder, it was mixed with 3% activated carbon, then the sample was put into an autoclave and 25 ml of ethanol was added and heated at  $200^\circ\text{C}$  for 20 hours, then sintered and tested for XRD, then made into a slurry and coated to obtain the width of  $\text{Na}_2\text{Li}_2\text{Ti}_6\text{O}_{14}$ .

The next stage is the synthesis of the LiNMC material. First, solution A is made containing  $\text{NiSO}_4 \cdot 6\text{H}_2\text{O}$ ,  $\text{MnSO}_4 \cdot \text{H}_2\text{O}$ , and  $\text{CoSO}_4 \cdot 7\text{H}_2\text{O}$  in the amount of 150 mL of distilled water in a beaker. Then, make solution B containing  $\text{Na}_2\text{CO}_3$  which is dissolved in 50 mL of distilled water in a beaker. After that, solution A and solution B are mixed slowly. Then, it is precipitated to produce metal carbonate precipitates. Then, the metal carbonate precipitate is filtered using filter paper with a Buchner funnel (while checking whether there is still sulfate by precipitating the filtered solution with  $\text{BaCl}_2$  solution until no  $\text{Ba}_2\text{SO}_4$  precipitate forms). Then, the metal carbonate precipitate is dried in an oven at temperature  $100^\circ\text{C}$  until dry. After that, milling was carried out between the metal carbonate precipitate and  $\text{C}_2\text{H}_2\text{O}_4 \cdot 2\text{H}_2\text{O}$  using ethanol solvent in a planetary ball mill at a speed of 1200 rpm for 6 hours. Then, milling was continued by adding LiOH as much as (excess 5%) for 4 hours. After that, the sample was transferred into a beaker and dried in an oven at a temperature of  $80^\circ\text{C}$  until dry. After drying, the sample was finely crushed and then sintering was carried out using a muffle furnace at a temperature of  $450^\circ\text{C}$  for 5 hours continued at  $850^\circ\text{C}$  for 16 hours at a ramp of  $5^\circ\text{C}/\text{minute}$ . The final stage is the fabrication of full cell coins for lithium ion batteries and pressing, then the batteries are tested using *charge-discharge*, *columbic efficiency*, *cyclic voltammetry* and *electrochemical impedance spectroscopy tests* to determine battery performance. .

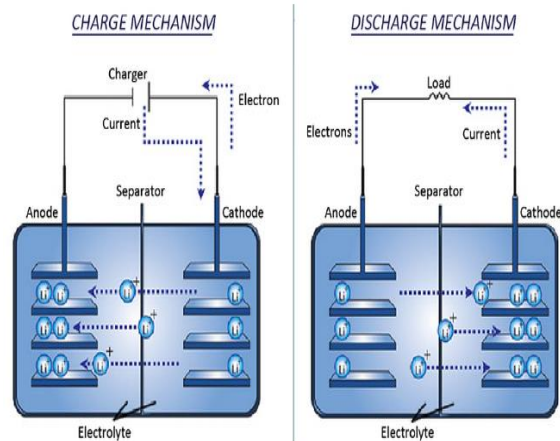


**Fig. 1.** Process of discharging and charging a lithium ion battery.

The anode material  $\text{Na}_2\text{Li}_2\text{Ti}_6\text{O}_{14}$  in this study is formed from several constituent materials as follows:

Titanium Oxide  $\text{TiO}_2$ , Lithium Carbonate  $\text{Li}_2\text{CO}_3$ , Sodium Bicarbonate  $\text{NaHCO}_3$ , Activated Carbon and Ethanol. The crystal phases that  $\text{TiO}_2$  has are anatase, rutile, and brookite. The material is widely used because it has high oxidative power and stability [10]. Lithium carbonate is an ionic bond with the formula  $\text{Li}_2\text{CO}_3$ , has a molar mass of 73.891 g/mol, a melting point of 723 °C and is soluble in water. Lithium carbonate's solubility in water is lower than other lithium substances. It decomposes at temperatures > 1300 °C. The surface tension at 800 °C is 241 mN/m.  $\text{NaHCO}_3$  is a chemical compound with the formula  $\text{NaHCO}_3$ . This compound belongs to the salt group [13]. Sodium bicarbonate has a molecular weight of 84.01 g/mol, with a density of 2.16 g/cm<sup>3</sup> melting point of 270°C and dissolves in water at 6.9g/100mL. Activated carbon is a material with an amorphous structure and a high level of porosity. Activated carbon has high performance in electrical conductivity and good thermal stability. These characteristics play an important role in its performance as an active material because it plays an important role in determining the performance of activated carbon in the absorbent process. Activated carbon is categorized as non-graphite because it has a low density and porous structure. Activated carbon does not dissolve in water, has a density of 1.8 - 2.1 g/cm<sup>3</sup>, melting point 3550 °C, with a PH of 5.0 – 10.0. Activated carbon is stable at room temperature but is sensitive to inertia [3]. Ethanol is a flammable compound and has a clear liquid and has a molecular weight of 46.07g/mol, a boiling point of 78.3 °C, a melting point of -114.5 °C, and a PH value of 7 in g/L in water at a temperature of 20°C. Ethanol is a polar solvent so it is often used to identify flavonoid compounds [9]. Ethanol can be made from agricultural materials, namely materials containing sugar, starch and cellulose [12].

The combination of particles through a diffusion process at high temperatures is often called sintering. In this event, there is shrinkage of components and growth of grains between particles that are close to each other so that a complex material is produced. This event can be seen based on the image below.

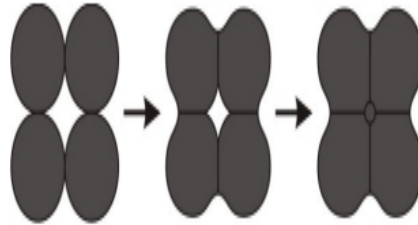


**Fig. 2.** Sintering process material

The diffusion process taking place and activating the energy source is called the sintering process. Physical properties can change along with the diffusion process after sintering, namely density, porosity, and shrinkage and enlargement of grains [5].

The x-ray diffraction method identifies the crystallinity phase so that the particle size is obtained, where the working principle is to shoot x-rays into the medium and then they will be scattered into the medium which is lower than the incident intensity. This causes the absorption of material and the scattering of atoms. In the same phase, the light rays reinforce each other, which is called x-ray diffraction, but in different phases, the light rays cancel each other out.

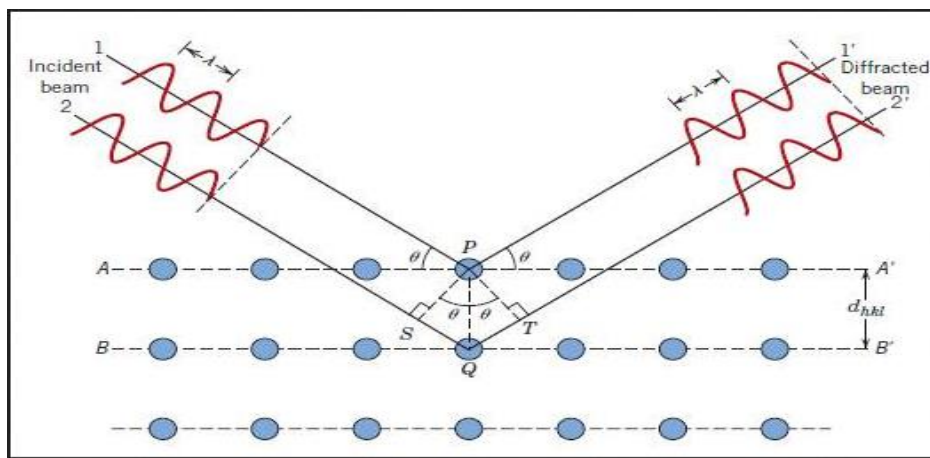


**Fig. 3.** X-ray diffraction

Based on Figure 3, the wavelength forms an hkl plane pattern with intensity measured as a function of the angle of reflection to the angle of incidence ( $2\theta$ ). Constructive interference can only occur if Bragg's law is fulfilled.

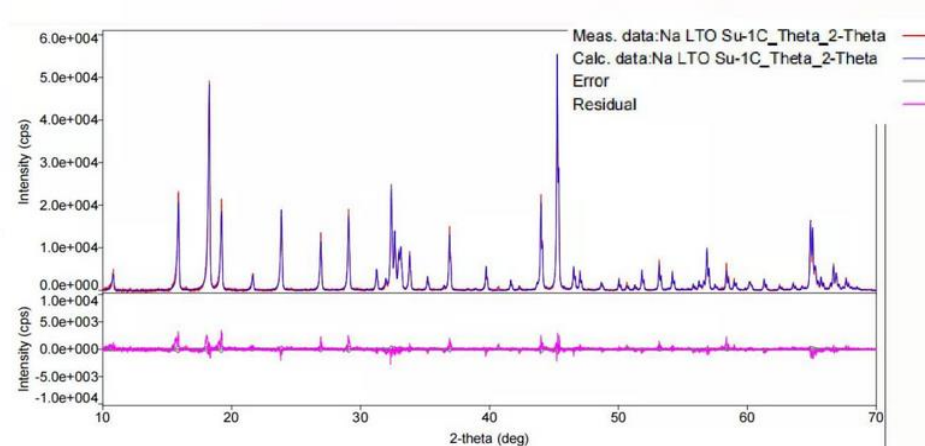
$$n\lambda = 2d \sin\theta \quad (1)$$

Where  $d$  is the distance between planes (hkl) and  $\sin \theta$  is the diffraction angle. Equation 1 is called Bragg's law with the critical angle  $\theta$  to fulfill this law known as the Bragg angle [1].

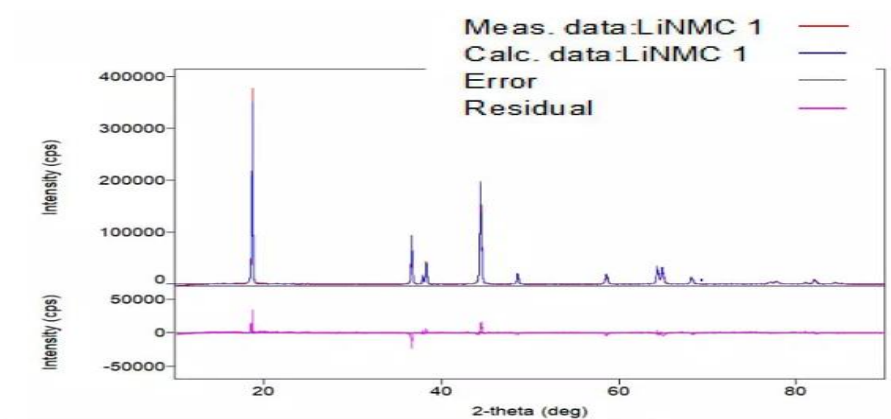
### 3 Results and discussion

#### 3.1 X-Ray Diffraction (XRD) analysis

The X-Ray Diffraction test is a method used to determine the crystal phase that is formed as a result of synthesis, where this tool uses x-rays as a medium which are fired at the sample at a certain angle. X-rays hit the sample and form a pattern according to the diffraction pattern that makes up the sample.



(a)



(b)

**Fig. 4.** X-Ray Diffraction Test Graph (a)  $\text{Na}_2\text{Li}_2\text{Ti}_6\text{O}_{14}$  material (b) LiMNC material

$\text{Na}_2\text{Li}_2\text{Ti}_6\text{O}_{14}$  anode material show sharp peaks so it has high crystallinity. It can be seen in image a that it is identified as having a crystal structure with the highest peak at  $2\theta = 45.2629^\circ$  with a plane distance of  $d = 1.9975 \text{ \AA}$  and has a cubic crystal structure. It has a density of  $1.17700 \text{ g/cm}^3$  with a lattice parameter of  $9.7399 \text{ \AA}$ , and has a crystal size of  $66.02571 \text{ nm}$ .

Based on observations of the crystal structure and phase results of the x-ray diffraction pattern for the NMC 811 cathode material, it was identified as having a crystal structure with the highest peak at  $2\theta = 41.934^\circ$  with a plane distance  $d = 4.7345 \text{ \AA}$  and having a crystal size of  $10.50409 \text{ nm}$ . It can also be seen that in the cathode material the peak obtained is sharp, this shows that the cathode material has high crystallinity. The LiNMC cathode material shows that the phase peaks are at angles  $2\theta = 36.67^\circ, 37.83^\circ, 38.32^\circ, 44.33^\circ, 48.58^\circ, 58.58^\circ, 64.30^\circ, 64.88^\circ, 68.08^\circ, 77.78^\circ,$  and  $81.85^\circ$  and have a crystalline structure cubic.

### 3.2 Cyclic Voltammetry (CV) analysis

Cyclic Voltammetry test was carried out at scan rate  $120 \mu\text{V/s}$ . The Cyclic Voltammetry test on the material  $\text{Na}_2\text{Li}_2\text{Ti}_6\text{O}_{14}$  determines the peak voltage of reduction and oxidation is carried out to determine the capacity of each in each process that occurs and determine whether an anode is reversible or not, as shown in the following graph:

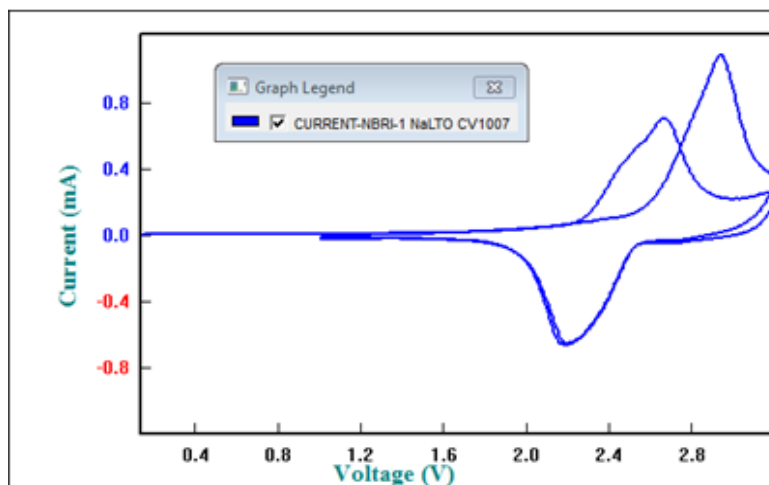


**Fig. 5.** Cyclic Voltammetry graph for  $\text{Na}_2\text{Li}_2\text{Ti}_6\text{O}_{14}$  and NMC811

Based on Figure 5, the oxidation reaction process occurs due to polarization. The CV test results show a relationship between charge potential and discharge potential so that it undergoes an oxidation and reduction process. Based on the CV test, look for the peaks of the anodic curve and cathodic curve, where the anodic curve is the area with negative current and the cathodic curve is the area with positive current. The peak value of the anodic potential in cycle 1 and cycle 2 can be seen in the following table:

**Table 1.** Cyclic Voltammetry Test of Lithium Ion Batteries in Full Coin Cells with NaLTO Anode and NMC811 Cathode.

Cycle	V <sub>oks</sub> (volt)	V <sub>red</sub> (volt)	V <sub>pol</sub> (volt)	I <sub>oks</sub> (mA)	I <sub>red</sub> (mA)
1	2.935	2.188	0.747	1.070	-0.662
2	2.659	2.192	0.467	0.694	-0.652

Table 1 shows the results of the CV test where the anodic potential peak at 1<sup>st</sup> cycle was 2,935 V and 2<sup>nd</sup> cycle was 2,659 V and the peak cathodic potential at 1<sup>st</sup> cycle was 2,188 V and 2<sup>nd</sup> cycle was 2,192 V. This shows that there is no such a significant change. Meanwhile, the current value obtained during the oxidation process of 1st cycle was 1,070 mA, on the 2nd cycle, it was -0.694 mA, and the reduction current during the 1st cycle was -0.662 mA, on the 2nd cycle, it was -0.652 mA. Based on the table above, the diffusion coefficient value was obtained. for oxidation of  $1.131 \times 10^{-12} \text{ cm}^2/\text{s}$  and reduction of  $9.105 \times 10^{-10} \text{ cm}^2/\text{s}$ .

The coulombic efficiency test was carried out to determine the resistance and capacity after repeated use of the battery. A graph of the coulombic efficiency data has been obtained as follows:

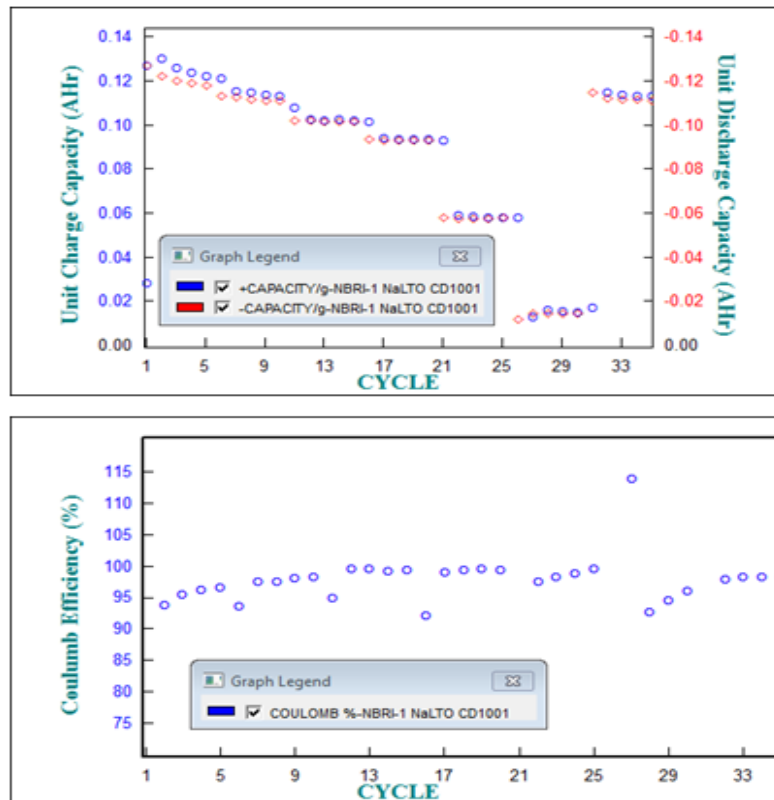


**Fig. 6.** Graph of coulombic efficiency for the first 5 cycles

Based on Figure 6, a *coulombic efficiency test* was carried out for the first 5 cycles where the results obtained were an increase in the *coulombic percent value*. The increase that occurs shows that battery performance is getting higher. The increase in *coulombic efficiency* values can be seen in the following table :

**Table 2** *Coulombic Efficiency* for the First 5 Cycles of Lithium Ion Batteries in Full Coin Cells with NaLTO Anode and NMC811 Cathode

Cycle	Capacity		Efficiency Coulomb (%)
	Charge (mAh/g)	Discharge (mAh/g)	
1	0.02797	0.12606	45.069
2	0.12931	0.12126	93.774
3	0.12524	0.11949	95.408
4	0.12303	0.11834	96.187
5	0.12169	0.11743	96.499

Based on table 2, it is known that the highest capacity value is in cycle 5 while the lowest capacity is in the first cycle. Meanwhile, the *coulombic efficiency* value in the first cycle is 45,069% or below 50%, so this causes an imbalance between the *charge-discharge process*. So the power in the battery is smaller. Meanwhile, in cycles 2-5, the *coulombic efficiency* values are close to 100%, namely 93.774%, 95.408%, 96.187%, and 96.499%. This shows that the battery has large energy storage capacity due to its high *coulombic efficiency value*

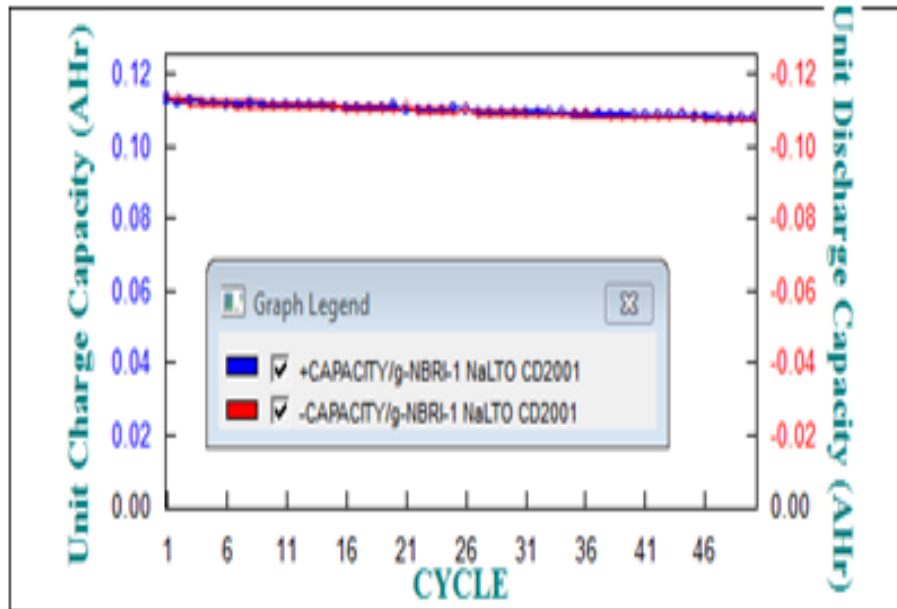


**Fig. 7.** *Coulombic efficiency* graph for 50x cycle



Based on Figure 7, the *coulombic efficiency graph* was tested for 1x and 50x cycles with a 1st capacity of 111.71 mAh/g after 50th of 107.16 mAh/g. Discharge on a 50x cycle is carried out in C/2 or equal to 2A with a time of 2 hours. This shows that the smaller the current, the longer it takes for the discharger .

**Table 3.** *Coulombic Efficiency* for 50x Cycle Lithium Ion Batteries in Full Coin Cells with NaLTO Anode and NMC811 Cathode

Cycle	Capacity		Efficiency Coulomb (%)
	Charge (mAh/g)	Discharge (mAh/g)	
1	111.71	111.80	100.08
50	107.16	106.65	99.52

*Coulombic Efficiency* value is 100.08%, while in the 50th cycle the *coulombic efficiency value* is 99.52%, there is a decrease but it is quite stable, and it has high energy storage capacity. Table 3 also shows that the capacity in cycle 1 is greater than in cycle 50, so the *coulombic efficiency value* is greater in cycle 1 than in cycle 50, so the power it has is even greater.

### 3.3 Charge-Discharge analysis

*Charge-discharge (CD)* testing aims to determine the performance of the battery to obtain the specific capacity of the battery at a certain *current rate* , namely the time required for the battery *Charge-Discharger process*. This *Charge-Discharger* test was carried out at a *current rate of C/10* . Charging a lithium ion battery with a current of 0.155mA can be seen in Figure 9 This current has a constant electric current graphic pattern. However, when the battery is *charged* approaches the maximum voltage, the current value will decrease to prevent *overcharging* . The *charge-discharge* test was carried out at a current of 0.15 mA and a potential range of 1.5-3.5V, based on this test, the specific capacity value for the *charging process* was 160 mAh/g and the specific *discharge capacity* was 120 mAh/g and the resulting *coulombic efficiency* was 70%

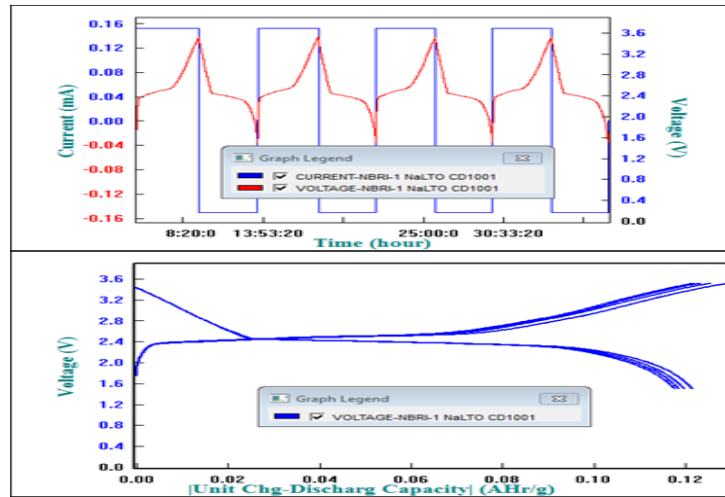


**Fig. 8.** Charge-Discharge Test Graph

### 3.4 Electrochemical Impedance Spectroscopy analysis

This test is carried out to measure the impedance of a material, by applying a sinusoidal AC signal from 2-10 mV. Based on the EIS test, it shows the electrical (conductive) properties of the electrolyte-electrolyte system of a battery.

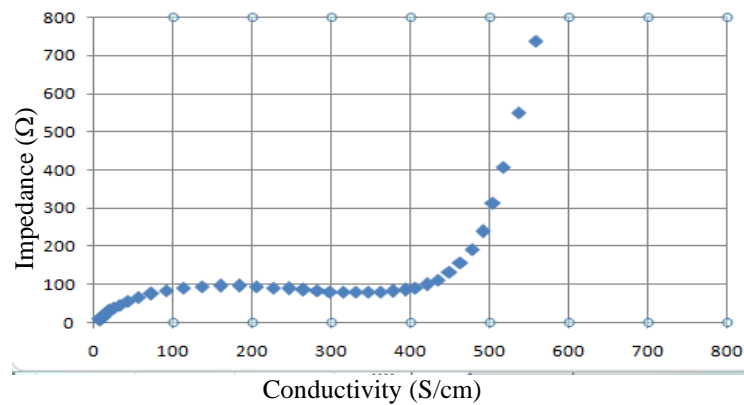


**Fig. 9.** EIS graph between impedance and conductivity

In Figure 9, a continuous EIS test graph is obtained. Based on this graph, it shows that the impedance is decreasing so that the conductivity of the battery is increasing. This shows that the capacitive properties of the battery are getting better. This is due to the resistance imposed on the sample. From the graph above, the conductivity value increases. So lithium-ion moves easily so that the charge density and mobility of lithium-ion are higher, this causes the conductivity value to be higher. The graph shows that the resistance is small so the conductivity value is large.

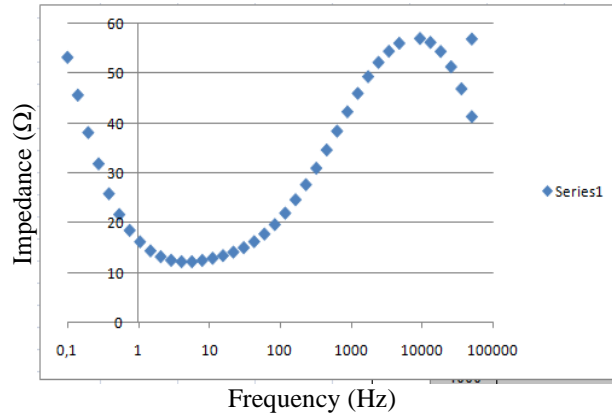


**Fig. 10.** EIS Test Graph Between Impedance and Frequency

Based on Figure 10, the graph between frequency and phase shows that the value for F1 is equal to 5.67 KHz, while for the value for F2 equal to 9.29 KHz, there is a large decrease in the resulting frequency value.

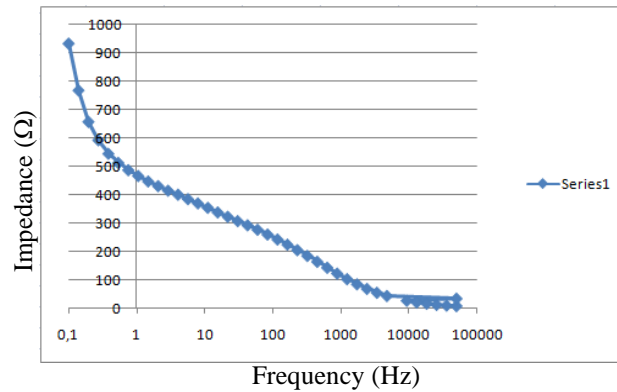


**Fig. 11.** EIS test graph between frequency and phase

Based on Figure 11, the graph between impedance and frequency shows that the impedance value is 377Ω at F, while at F<sup>2</sup> the impedance value is 15.34Ω. This proves that the greater the impedance value, the smaller the frequency value. The EIS test results can determine how much conductivity the material has in a Full Cell lithium ion battery with a NaLTO anode and an NMC811 cathode using the following formula.

$$\sigma_{total} = \sigma_e + \sigma_{ct} \quad (2)$$

Where,  $\sigma$  is electrical conductivity (S/cm), R is resistance (Ω), t is the thickness of the anode sample (cm) and A is the surface area of the anode sample (cm<sup>2</sup>). Can be seen in the following table:

**Table 4** Material Conductivity Values for Lithium Ion Batteries in Full Coin Cells with NaLTO Anode and NMC811 Cathode.

Re ( $\Omega$ )	R <sub>ct</sub> ( $\Omega$ )	$\sigma_e$ (S/cm)	$\sigma_{ct}$ (S/cm)	Thick (cm)	Area (A) (cm <sup>2</sup> )	$\sigma_{tot}$ (S/cm)
6.8455	377.172	44.993 x 10 <sup>-5</sup>	81.660 10 <sup>-5</sup>	0.0062	2.0069	126.653 x 10 <sup>-5</sup>

Based on table 4, the material conductivity value for a lithium ion battery in a full coin cell with a NaLTO anode and an NMC811 cathode is  $126,635 \times 10^{-5}$  S/cm, where the sample has an electronic resistance value of 68,455  $\Omega$  and an ionic resistance value of 377,172  $\Omega$ .

#### 4 Conclusion

Based on the XRD test, the materials Na<sub>2</sub>Li<sub>2</sub>Ti<sub>6</sub>O<sub>14</sub> and NMC811 both have a cubic crystal structure and have high crystallinity, where Na<sub>2</sub>Li<sub>2</sub>Ti<sub>6</sub>O<sub>14</sub> has a crystal size of 66.02571 nm and NMC811 has a crystal size of 10.50409 nm. Based on the Coulombic efficiency test, it was found that the efficiency value was 96.50% in the first 5 cycles and for the 50x cycle it was 99.52%, this shows that the battery storage capacity is getting higher. Meanwhile, the charge-discharge test proved that the higher the current, the shorter the time taken to reach the maximum voltage. Based on the EIS test, the greater the frequency, the smaller the resulting impedance and a conductivity value of  $126.64 \times 10^{-5}$  S/cm is obtained.

It is recommended that the slurry be made more carefully so that the materials used do not become lumpy during coating, pay more attention to the assembling process, and understand more about the milling and sintering processes.

#### Acknowledgements

This research was supported by supervisor of Sriwijaya University, technical staff XRD from Research Center of Physics

#### References

- [1] Afza, E.: Making Ba-Hexa Ferrite (BaO.6Fe<sub>2</sub>O<sub>3</sub>) Permanent Magnets Using the Coprecipitation Method and Its Characterization. [Thesis]. Medan: University of North Sumatra. pp. 25-65 (2011)
- [2] Andre, S.J., Kim, P., Lamp, SF., Lux, F. Maglia: Future generations of cathode materials: an automotive industry perspective. Journal of Materials Chemistry A. Vol. 3(13). pp. 6709–6732 (2015)
- [3] Lubis, RAF et al.: Production of Activated Carbon from Natural Sources for Water Purification. Chemical Science and Technology. Vol 2(3). pp. 67-73 (2020)
- [4] Ramlan., Bama. A.A. : Effect of Sintering Temperature and Time on the Properties of Porcelain Materials for Solid Electrolyte Materials (Electrolyte Components). Science Research. Vol 3(14). pp.1-4 (2011)

- [5] Ramlan., Johan.A.: Identification of Na-β"-Al<sub>2</sub>O<sub>3</sub> Ceramic, with the Addition of Composition Variations (0%, 3% and 6%) MgO Weight. *Journal of Scientific Research*. Vol 1(12). pp. 1-6 (2009).
- [6] Raihan, A.Z.: Synthesis and Characterization of LiNi<sub>0.6</sub>Co<sub>0.2</sub>Mn<sub>0.2</sub>O<sub>2</sub> and LiNi<sub>0.8</sub>Co<sub>0.1</sub>Mn<sub>0.1</sub>O<sub>2</sub> Using the Solid State Method for Lithium Ion Battery Cathode. [Thesis]. pp . 67-88 (2020)
- [7] Shu, J., Wu, K., Wang, P., Lin, X., Shao, L., Wang, D.: Lithiation And Delithiation Behavior Of Sofium Lithium Titanate Anode. *Electrochimica Acta* 173. pp. 595-606 (2015)
- [8] Myung, S.T., Maglia, F., Park, K.J.: Nickel-Rich Layered Cathode Materials for Automotive Lithium-Ion Batteries: Achievements and Perspectives. *ACS Energy Letters*. Vol. 2, (1). pp. 196 – 223 (2016)
- [9] Suhendra, CP, et al.: Effect of Ethanol Concentration on the Antioxidant Activity of Ilang Rhizome Extract (*Imperata Cylindrica* (L) Beauv.) in Extraction Using Ultrasonic Waves. *Journal of food science and technology*. Vol 1(8). pp. 27-30 (2019)
- [10] Syukri., Dahlan, D., Agustina, E., : Structure and Optical Coating of TiO<sub>2</sub> (Titanium Oxide) Thin Films Produced Using the Electrodeposition Method. *Unand Journal of Physics*. Vol 3(2). pp. 2302-8491 (2013).
- [11] Ohzuku, T. and Makimura, Y.: Layered Lithium Insertion Material of LiCo<sub>1/3</sub>Ni<sub>1/3</sub>Mn<sub>1/3</sub>O<sub>2</sub> for Lithium-Ion Batteries. *Chemistry Letters*. Vol. 30(7). pp. 642-643 (2001)
- [12] Utami, L.: Making Ethanol from Noni Fruit. *Journal of chemical engineering*. Vol 1(4). 225-259 (2009)
- [13] Yulianti, L., Wahyudi, S., Marlina, E.: Production of Brown's Gas from Electrolysis of H<sub>2</sub>O with NaHCO<sub>3</sub> Catalyst .*Mechanical Engineering Journal*. Vol 1(4) pp. 53-58 (2013)